RESEARCH PAPER | Engineering | Volume : 3 | Issue : 12 | Dec 2013 | ISSN - 2249-555X

Characterization of MEMS Three-Direction Capacitive Accelerometer

KEYWORDS

Mrs. Anitha Bontha
Assistant Professors in Department of ECE , VelTech Dr. RR & Dr.SR Technical University, Avadi

Mr. Amit Kumar Sinha
Assistant Professors in Department of ECE , VelTech Dr. RR & Dr.SR Technical University, Avadi

Mr. Shailendra Kumar Mishra
Assistant Professors in Department of ECE , VelTech Dr. RR & Dr.SR Technical University, Avadi

Mr. Gaddam Vinay
Assistant Professors in Department of ECE , VelTech Dr. RR & Dr.SR Technical University, Avadi

ABSTRACT *In this project we present the design and fabrication of a MEMS three-direction capacitive accelerometer. The design of the motion sensor includes sensing acceleration in the x-, y-, and z- directions, tilting, and free-fall. This device achieves this function implementing four serpentine spring systems suspending a proof-mass. The structure of the sensor can then be modeled as a mechanical mass-spring system where the mass is one side of a parallel plate capacitor and the frame of the accelerometer is the other. The device then has a nominal capacitance and will change as the proof-mass responds to acceleration events. These changes can be monitored along each axis and then analyzed to provide information on the motion occurring.*

The design features a proof-mass with interdigitated fingers along each side that correspond to interdigitated fingers extending from the frame. This structure then creates many small Parallel plate capacitors that will sense motions in-plane with the x- and y- axes. Beneath the Proof-mass, separated by an air gap, is the bottom electrode acting as one parallel plate of the Differential capacitor sensing along the z-axis.

1. Introduction

Motion detection is mainly achieved with accelerometers. The MEMS structures within a package respond to motion events through bending, flexing, or somehow altering their structures just as a cantilever beam or spring system behaves in the realworld scale. This, in turn, changes the value within some electrical interface component of the design allowing for measurement to take place. MEMS design and fabrication techniques are used to realize these devices.

There are several different types of accelerometers that differ in their method of sensing movement. These include capacitive, piezoelectric, piezoresistive and thermal [6, 7]. The thermal type accelerometers use a gas producing material within an enclosed package. There are then at least four temperature sensors arranged in the four corners of the device and one directly over the gas producing material itself. These types function by comparing the values from the temperature sensors to determine the orientation of the device. The more common types of accelerometers use capacitive techniques. The function is that a suspended proof mass acts as one plate of a parallel plate capacitor while the plate is stationary. The suspended proof mass deflects with motion, much like a spring, and changes the distance between the parallel plates. This then changes the value of the capacitor and allows interface circuitry to detect the difference and then calculate the force of the acceleration event. Many of these capacitive types are fabricated using Silicon on Insulator (SOI) techniques that provide a suitable platform for the silicon device, comprising the accelerometer, to be fabricated upon. It is important that the substrate the device is on is an insulator so that the capacitance values are not interfered with on the package itself .

The accelerometer presented in our design, fabrication, and analysis is of the capacitive sensing type.

There are many techniques to realizing three directions of motion which may include separate accelerometers oriented for each axis [6]. Our design features interdigitated sensing capacitors. These capacitors, or fins, extend from a proof mass suspended by a serpentine spring structure. While interdigitated fins for sensing are a common technique used in MEMS accelerometers, the actuation technique differs [7, 8, 9, 10]. As mentioned before, our proposed design encompasses all three directions of motion using a proof mass suspended by serpentine springs. Other techniques for achieving actuation include folded flexures, looped springs, or cantilever beams [11, 12, 13]

Aside from design and fabrication of MEMS devices, another daunting challenge is processing the actual signals, or data, provided by the devices. The challenge is that these devices are so small that the signals being monitored are extremely small as well. This makes it challenging to detect even smaller changes and convert the analog signal into a digital signal that can be analyzed. In our sensor, the femtofarad range capacitances need to be monitored while avoiding parasitic capacitances that will skew the data being provided from the MEMS sensor itself. The work presented here does not tackle the conversion of the capacitance values into a digital signal and is part of a separate research topic.

We designed, modeled, fabricated, and tested our MEMS capacitive accelerometers using various tools including AutoCAD for mask design, COMSOL Multiphysics for modeling, and implemented the Silicon on Glass (SOG) process at the Lurie Nanofabrication Facility (LNF) within the University of Michigan. The process for developing a MEMS device is expansive and begins with design. Once a particular method is decided that will be the sensing element of the accelerometer, the process steps for fabrication need to be established. In order to implement the SOG process steps, the proper masks for each layer of the device need to be carefully designed with incredible precision. Verification of the design is necessary and done in COMSOL Multiphysics where different simulations are executed. This includes vibrational, electrostatic, and modal analysis. Finally, testing of the fabricated

Volume : 3 | Issue : 12 | Dec 2013 | ISSN - 2249-555X

devices themselves becomes another challenge in itself and must be painstakingly consistent. Specialized tools are needed to handle the MEMS devices to ensure accuracy and safety of the devices. These include a clean room environment, probe station, wedge wire bonder, and the instruments to measure various electrical characteristics of the device.

2. Proposed Design

Our proposed MEMS capacitive accelerometer design features a proof mass suspended by serpentine spring structures, shown in Figure 1. The entire package is 2mm x 2mm x 100μm with a critical dimension of 10μm. It should be noted that each device is assumed to be 100μm thick because that is the given thickness of the silicon wafer used for processing. This spring structure was chosen to provide the greatest flexibility and allow for maximum displacement of the proof mass and sensing regions. Other designs were considered and included spiral spring types as well as traditional spring types. The capacitor fins extending from the proof mass are 200μm x 10μm. The proof mass itself is 395μm x 395μm featuring forty-nine 20μm x 20μm damping holes. Each side of the proof mass features five fins interdigitated with an opposing six anchored fins extending from the sides of the package.

It is important to note that this structure is made of doped silicon and is conductive. This is an important concept for the design because regions need to be isolated from each other to avoid short circuits during electrical measurements and testing. The proof mass and spring structures are isolated from the other components because the interdigitated fins and proof mass itself are part of parallel plate capacitors for sensing. If they were not isolated and were touching other components, the parallel plate capacitor would short circuit prohibiting proper function.

Other areas that require isolation include the bottom electrode and its associated contact pads. It is crucial that the silicon structure be suspended over the bottom electrode for the same reason the proof mass and fins need to be separated from the anchor fins. For clarity, each anchored fin section must be individually isolated as well to prevent shorting and ensure functionality.

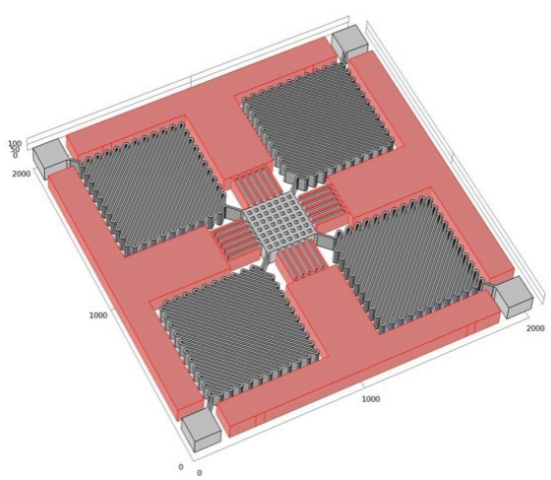

Figure 1: Three dimensional model of MEMS capacitive accelerometer demonstrating serpentine springs, proof mass, and interdigitated fin structures.

The sensing mechanism produces a capacitance that will serve as the raw output data for the system. It is important to understand the nominal capacitance while the entire system is at rest. Since the device behaves as a simple parallel-plate capacitor,it can be realized with Equation1.

$C = \epsilon A/d$ .....(1)

This shows that the capacitance of a region, C, is equal to the dielectric constant of air, ε, multiplied by the area of the overlapping sensing regions, A, divided by the distance separating the two sensing regions, d. For an interdigitated fins section, there are eleven small differential capacitors that dominate the sensing for the x- and y- axes. The actual area overlapping per set of differential capacitors is 180μm x 100μm separated a distance of 10μm. For an individual pair of interdigitated fins, the nominal capacitance is 15.9 femtofarads. For a set of eleven, the capacitance is 175.4 femtofarads. The entire sensing system composed of all four sets of interdigitated fins is 701.2 femtofarads.

The remaining sensing region is in the z-direction and is composed of the parallel plate capacitance formed between the bottom electrode and the suspended proof mass with damping holes. There are forty-nine 20μm x 20μm damping holes that must be removed from the area capacitance of the proof mass. This nominal capacitance is calculated to be 303.7 femtofarads, separated by a distance of 3μm.

Aforementioned was the explanation of the serpentine spring structure with emphasis on flexibility in all axes of motion. The air gap for the z-sensing region is set to 3μm for a particular reason. The SOG process developed at the LNF calls for an etching step with a hazardous solution, Hydrofluoric acid. This solution etches the glass at a certain rate and creates a tapered slope from the bottom of the recess created to the original planar surface of the glass wafer. It has been found that this depth creates a repeatable, reliable etch that allows the deposited bottom electrode to extend from the recess, up the tapered slope, and to the original surface with uniformity. If etched too long, uniformity is sacrificed and the bottom electrode deposition may not be successful.

The bottom electrode itself has been purposefully designed in such a way to focus the dominant sensing capacitances in their appropriate regions. Since parallel plate capacitors only create a value for regions that are overlapping, it does not make sense to coat the entire glass recess with metal. Also, there are very small capacitances formed between the bottom electrode and the overlapping serpentine spring structures. By minimizing the area of the region extending from beneath the proof mass to its contact pad that is outside the recess, the capacitances are further minimized. The bottom electrode extends symmetrically to each of its contact pads to maintain the devices symmetry and provide four distinct chances at measuring the z-capacitance in case some regions of the bottom electrode not protected by silicon during a Deep Reactive Ion Etching (DRIE) process step were damaged.

The 20μm pin holes serve an important purpose as well. During a z-motion event, air molecules are forced out and away from the proof mass that is oscillating back and forth over the bottom electrode. In such small scales, such as MEMS systems, air molecules are rather large and are difficult to move. These pin holes provide another route for air to escape during z-motion events so that the proof mass is able to be displaced without resistance due to displacing air molecules.

2.1 Modeling

After initial design, Finite Element Analysis (FEA) modeling was used. COMSOL Multiphysics was implemented to do such analysis. The models were imported from AutoCAD and physics models were applied in the FEA software. The model was then manipulated for simplicity while keeping all the same structural characteristics and is shown in Figure 2 [14]. In Table 1 the material properties and geometric parameters are shown that are used throughout the COMSOL simulations.

Volume : 3 | Issue : 12 | Dec 2013 | ISSN - 2249-555X

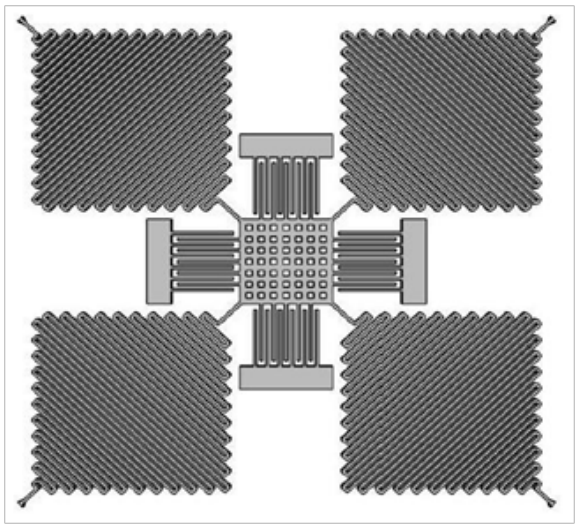

Figure 2: Simplified CAD model of accelerometer structure. Table 1: Parameters and material properties used in COMSOL Simulations.

Parameter	Value	Unit
Area of Accelerometer	2000×2000	μm^2
Area of proof-mass	395×395	μm^2
Thickness of proof-mass	100	µm
Young modules of silicon	1.67×10^{11}	N/m^2
Poisson ratio of the silicon	0.3	
Density of Silicon	2300	Kg/m^3
Relative permittivity of silicon	11.9	
Viscosity of air at 25°	1.1839×10^{-5}	Pa.s
Mean free path of air at 25°	6.78×10^{-8}	m
Relative permittivity of air	1	

Simulations performed include modeling of the air dampening effect during a z-motion event, maximum deflection in x- or y- directions, von mises stress analysis of serpentine springs, modal analysis, change of capacitance due to deflection, and electrostatic potential analysis of the device in sensing regions [14]. The values achieved during these simulations are shown in Figure 3.

It was found, as expected, that the presence of air molecules would damp the behavior of the motion during a z-motion event. The more air molecules to displace, higher pressures, relates to a greater damped motion. It was discovered that it would be beneficial to damp our motion because the initial event shows very similar maximum displacements. To avoid what seems to be a harmonic oscillation and continuously changing capacitance values, the presence of air molecules and removing damping holes from the design would be advantageous. The von mises stress analysis was performed to identify the problem regions of the spring design during large acceleration events. The spring design accommodates for stresses up to +-5 g and limits areas of elevated stress. The capacitance of the device itself as a function of displacement is crucial as well and was simulated up to 2.5µm. Modal analysis was used to identify resonance within the structure at certain frequencies. Resonance frequencies were found to be 2 kHz along the x-, y-, and z-axes. Finally, electrostatic potential was analyzed to verify that these forces would allow for displacement and therefore change in capacitance that would serve as the data to be processed from the device.

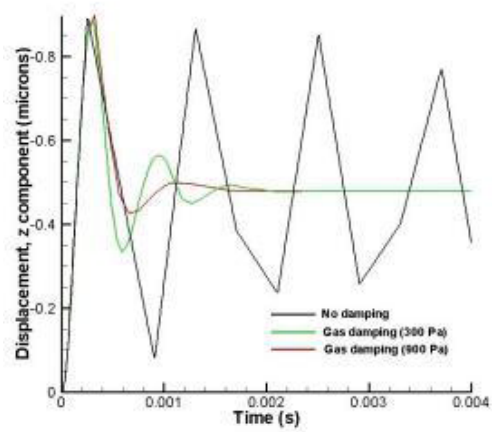

A

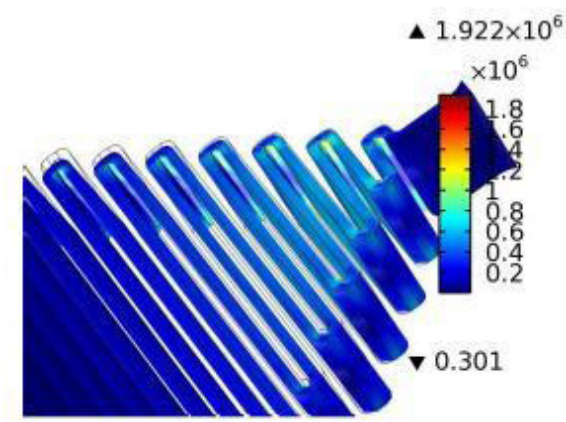

B

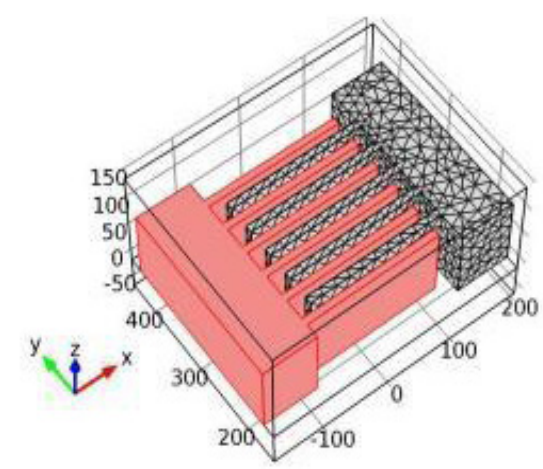

C

Volume : 3 | Issue : 12 | Dec 2013 | ISSN - 2249-555X

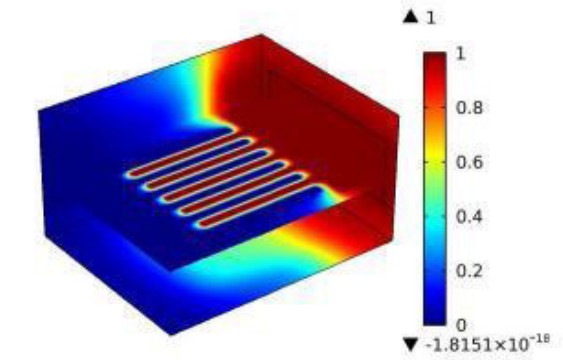

D

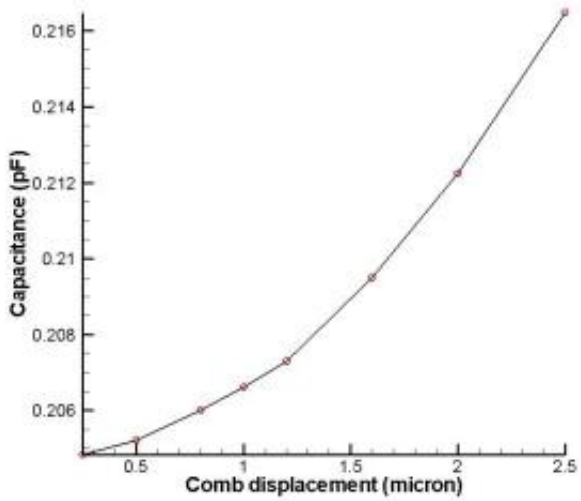

E

Order	Resonant frequency (Hz)	Mode shapes
1&2	1280	Vibrating by x or y axis (In-plane mode)
3	1838	Vibrating in z axis (out-of-plane mode)
4	1953	Vibrating along z axis (rotational mode)
5	39105	Vibrating along y or x axis (rotational mode)

F

Figure 3: (A) Results of modeling air dampening in z-motion event for different pressures.
(B) Von mises stress analysis of serpentine spring structure.
(C) Model used preparing electrostatic testing and change in capacitance due to deflection.
(D) Electric potential of sensing fin region.
(E) Change in capacitance as a function of displacement.
(F) Values obtained during modal analysis along each axis in and out-of-plane.

2.2 Fabrication

The next great challenge comes in the form of the actual fabrication of these devices. Achieving precise, controlled structures on the order of just a few microns requires a great deal of resources and understanding. It is important to perform these processing steps in an environment that will eliminate particles in the air that may destroy the functionality of the devices being fabricated. The SOG process developed by the LNF provides the steps necessary in achieving suspended silicon structures on the sub-micron scale. A cut-view of a finalized sample created using the SOG process is shown in Figure 4. It should be noted that there is a glass recess with an electrode deposited that extends from the recess to the original surface of the glass wafer and that the silicon is suspended over the recess with an air gap of 3μm below.

Figure 4: Cut-view of finished SOG structure.

The SOG process can be summarized by examining each processing step required. A bare 4" glass wafer 500μm thick is used as the substrate for the process. A chrome layer is deposited to serve as a mask layer for a later processing step. Photolithography is then performed to pattern photoresist in the glass recess pattern. After developing the photoresist, the exposed areas of chrome are etched away exposing the original glass surface in a pattern consistent with the glass recess.

A hydrofluoric acid solution is used to etch away the exposed areas of glass. The photoresist and chrome are then stripped away revealing the original glass wafer with recesses. Photolithography is then performed again to patter for the bottom electrode metal. The photoresist is then developed to realize the bottom electrode pattern. Using e-beam evaporation techniques again, a chrome and platinum layer is deposited across the entire wafer. This is important because a lift-off technique will be used to reveal the bottom electrode metal in its intended pattern at the bottom of the recess extending outward. Since the metal is deposited over all surfaces, the exposed glass where photoresist has been developed away and on top of the photoresist itself, the acetone bath to strip the photoresist also eliminates the metal on top as well. The sample is now a bare glass wafer with the bottom electrode patterned in the recesses of the glass extending outward.

Photo resist is spun onto the entire sample to protect it during the next processing step. Pre-dicing is necessary so that once fabrication is finished; each individual device can be separated from the rest of the wafer. The dicing tool cuts at 250μm, halfway through the glass wafer, and is then stripped of its photoresist and cleaned. The silicon wafer is then fused to the glass wafer using a process called anodic bonding.

Now that the 4" silicon wafer is bonded to the glass wafer, deposition of the chrome and gold metal pads on top of the device can be performed. Photolithography is then performed to pattern for the metal pads. The gold is etched away followed by a chrome etch. This leaves the patterned metal pads on top of the silicon wafer. The photoresist is then stripped and photolithography is performed again to pattern the DRIE pattern that will define our silicon structures.

After patterning the photoresist for the final processing step, the sample is placed within the DRIE chamber. A Bosch DRIE instrument etches away the silicon revealing our final structures. The remaining photoresist is stripped away in the DRIE chamber and the final product is ready for testing. Photographs have been taken during various processing steps and

Volume : 3 | Issue : 12 | Dec 2013 | ISSN - 2249-555X

are shown in Figure 5.

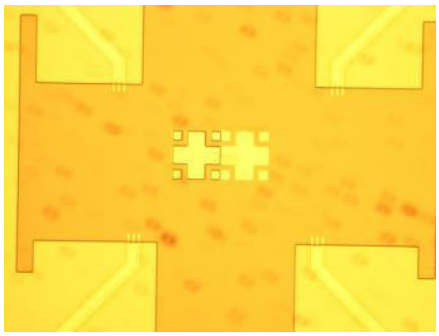

A

B

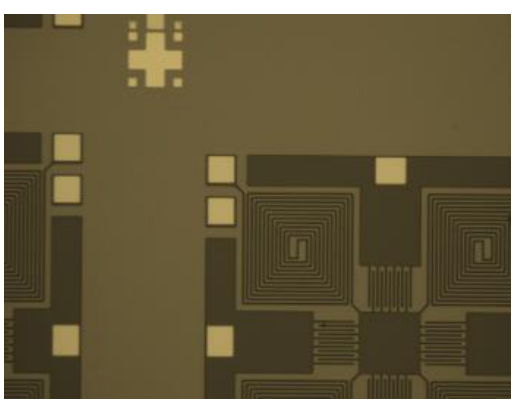

C

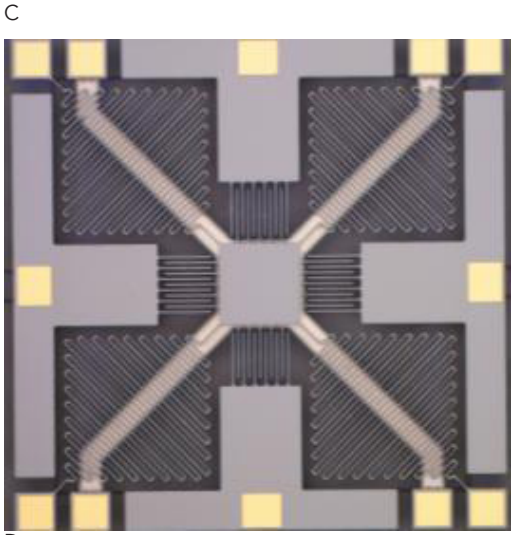

D

Figure 5:
(A) Optical microscopy of glass recess with bottom electrode deposition and alignment marks.
(B) Optical microscopy of bottom electrode fingers extending from recess up onto initial glass surface.
(C) Optical microscopy after wafer bonding, metal pad deposition, and DRIE photolithography.
(D) Optical microscopy of final MEMS Accelerometer structure.

After completion of the processing run, scanning electron microscopy was performed to examine the structures closely, shown in Figure 6. An SEM image was taken of a device that was lost after a dicing step due to an immense vibrational shock.

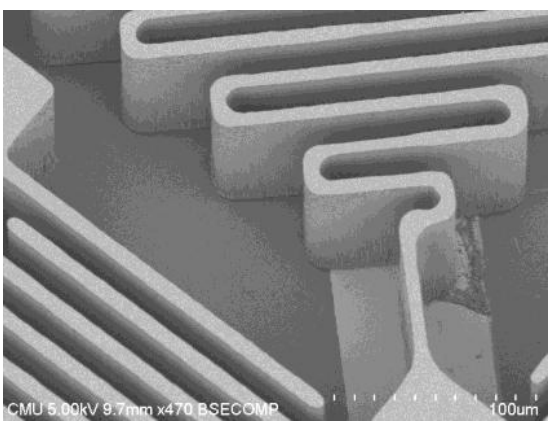

A

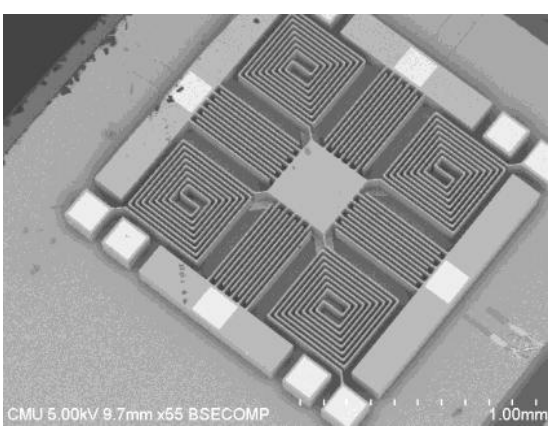

B

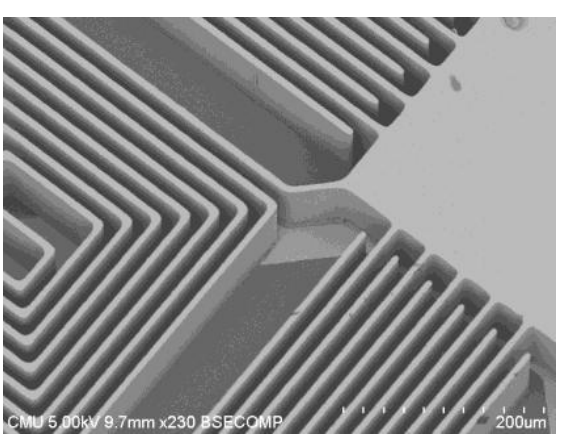

C

Volume : 3 | Issue : 12 | Dec 2013 | ISSN - 2249-555X

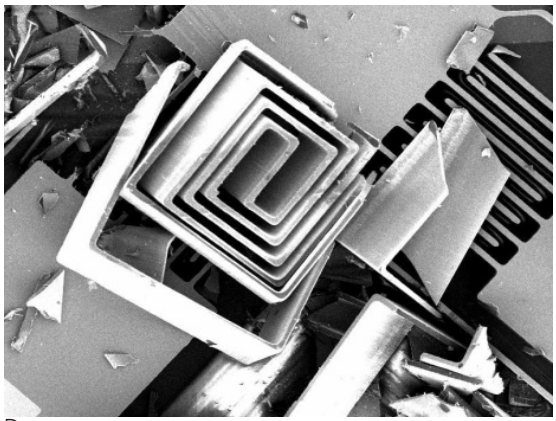

D

Figure 6:
(A) SEM image of serpentine spring structure.
(B) SEM isometric view of MEMS accelerometer.
(C) Zoomed SEM isometric view of sensing and spring regions.
(D) SEM image of an accelerometer destroyed during a vibrational shock.

In order for these various steps of photolithography to occur, the appropriate mask needs to be applied and aligned correctly, shown in Figure 7. The first mask needed defines the glass recesses and features an alignment mark. This mask also features a critical property that creates a venting channel that extends to the edges of the wafer so provide pressure equalization during other processing steps that pull a vacuum on the sample. The next mask must align to the marks created during the first photolithography step and provide another for the next step and is the bottom electrode mask. After bonding the silicon wafer, it becomes challenging to align samples.

The next mask was designed to accommodate for backside alignment for the sample. This maskis for the metal pads on top of the silicon and has alignment marks that will fit inside the

previous alignment marks. Previously, the alignment marks became slightly larger so that they could be visible during alignment with microscopes. It is crucial in the design that the metal pads. align directly over top of the portion of bottom electrode that extends outside of the glass recess. Finally, the DRIE mask is created for traditional alignment and defines the areas of silicon that comprise our device.

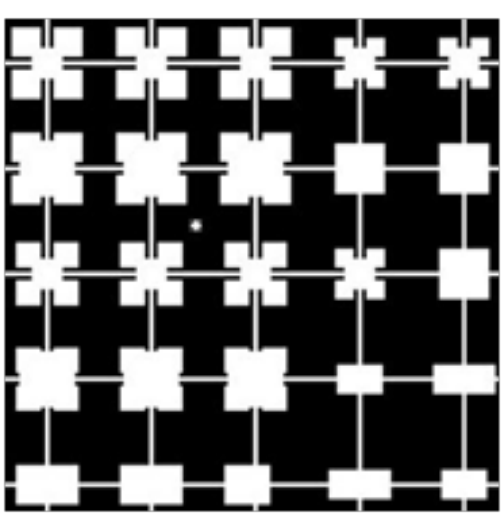

RECESS

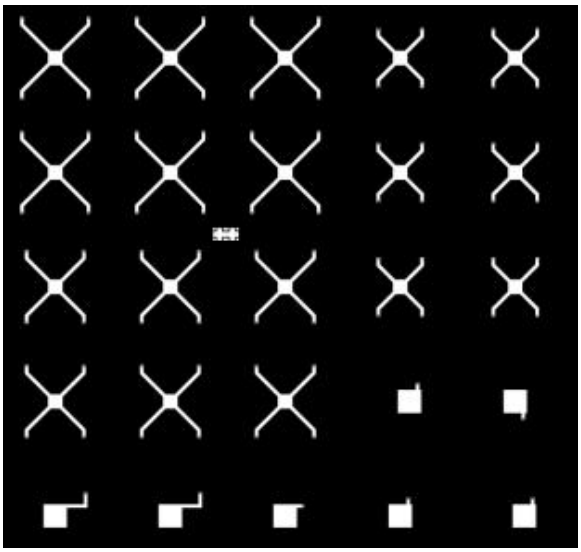

METAL

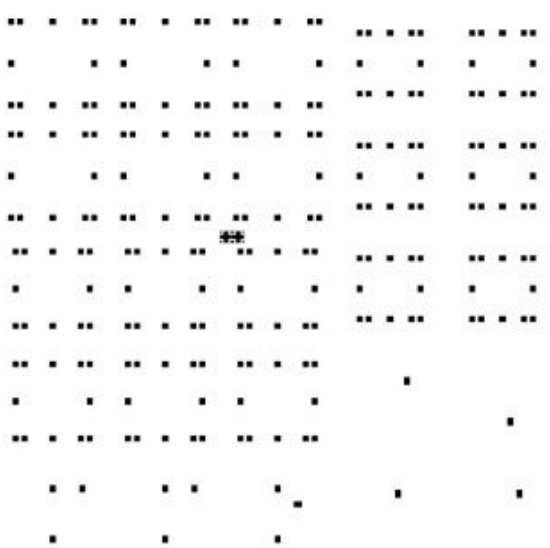

PADS

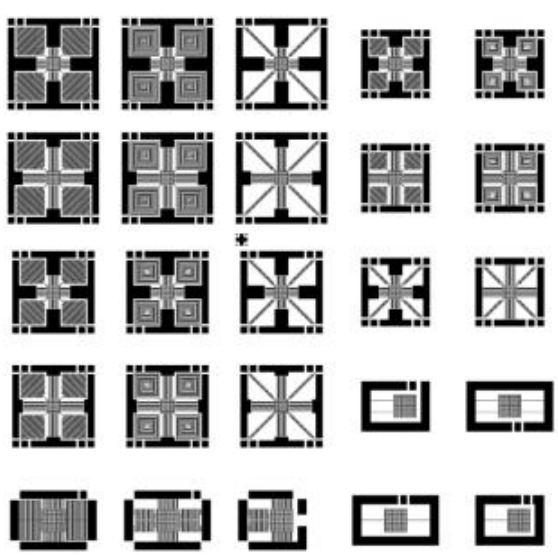

DRIE

Volume : 3 | Issue : 12 | Dec 2013 | ISSN - 2249-555X

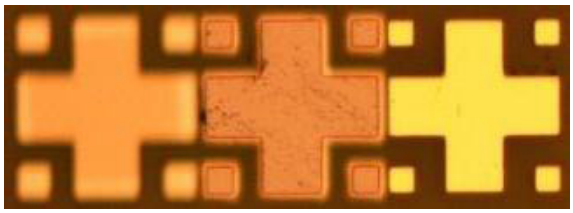

Figure 7: Mask layout and design for an individual die for each mask layer of SOG process showing alignment marks below.

3. Results

After successful fabrication of the MEMS 3-direction accelerometers, initial tests were conducted to verify their function. Using a probe station, shown in Figure 8, probe tips could be micro-positioned to create electrical contacts with each of the various pads of the devices. These shielded probe tips would be then connected to various measuring instruments. An ohmmeter was used to perform a short circuit test. This would ensure that regions of the accelerometer are not electrically connected, through the doped silicon structure, and create a short. This test is also useful for verifying that some regions that should be shorted, in fact are connected and that the resistivity is low. For example, in the very corners of the device are the pads that are connected.

The other instrument that is used during these static tests is a capacitance meter. A GLK capacitance meter with +- 2 femtofarad resolution was used to take capacitance measurements.

The probe tips are repositioned to measure the capacitance of the various sensing regions of the MEMS accelerometer. By placing a probe tip on a spring and proof mass pad while placing to the spring and proof mass structures. Placing the probe tips in any combination of these four corners should indicate a short circuit and provide a resistance reading on the ohmmeter that is very low. On the other hand, touching a corner pad and any other pad that is not in a corner should indicate an open circuit. This is expected because the spring and proof mass structure should not be touching any other component of the device. The ohmmeter would read that there is an overflow or resistance so great that there is essentially no connection. If a reading is made, it can be concluded that the spring proof mass structure is touching somewhere it should not and is discarded.

The other instrument that is used during the static tests is a capacitance meter. A GLK capacitance meter with +- 2 femtofarad resolution was used to take capacitance measurements. The probe tips are repositioned to measure the capacitance of the various sensing regions of the MEMS accelerometer. By placing a probe tip on a spring and proof mass pad while placing another on a bottom electrode pad will provide data for the z-direction capacitance that is being sensed by the device. On the other hand, by placing a probe tip on a spring and proof mass pad while placing the other on an anchor fin pad will provide a capacitance reading for that sensing region of interdigitated fins.

Future tests will include an electrostatic measurement to measure the deflection of the proof mass and therefore the change in capacitance achieved. This test will require a DC power source, voltmeter, capacitance meter, and camera system. While electrostatically charging the various regions of the device, deflection will occur in the proof mass. The camera will capture this motion and image processing will calculate the deflection achieved while the capacitance meter will output the real time capacitance and be logged using LabVIEW. The final tests will be of a dynamic nature and will require packaging of individual accelerometer devices so that they may interface with measuring equipment while in motion. This will require the wedge wire bonder and a vibration table. The vibration table will be driven by a sinusoidal voltage which will dictate the amplitude and frequency of the actual vibration achieved on the table. The real time capacitance will be changing due to the proof mass deflecting because of the acceleration of the vibration and will be captured using LabVIEW. another on a bottom electrode pad will provide data for the z-direction capacitance that is being sensed by the device. On the other hand, by placing a probe tip on a spring and proof mass pad while placing the other on an anchor fin pad

4. Relevance to Engineering Education

This research has had a tremendous impact on furthering the understanding of concepts learned during the pursuit of a degree in electrical engineering. The inherent design of the MEMS accelerometer requires a special understanding of capacitances, rigorous design specifications set forth by the SOG process, and understanding of interfacing with the components of the MEMS device. Aside from the mathematical development achieved during the course of this research, clear, concise, and direct communication was enhanced. It is essential that the ability to communicate a technical perspective when discussing design or troubleshooting a problem is established. Participating in this research not only required understanding of electrical engineering concepts, but mechanical engineering concepts as well. The CAD design of the masks needed for the SOG process required an acute attention to detail in drawings that are less than a micron in size. Cantilever and spring structures were analyzed and optimized to increase performance. Even an understanding of the chemical properties of solutions and processes used during the fabrication of these devices were required. Research of this type is incredibly unique because it is multidisciplinary and provides the opportunity to develop many technical and non-technical skills in an academic setting.

REFERENCE Ambron, S.(1990) . "Multimedia" in Ambron, S. and Hooper, K. (eds.) Learning with Interactive Multimedia: Developing Tools in Education, Microsoft Press, Redmond. | Anita Rastogi and Babita Parashar (2009), "Effective of e learning content in learning concept and teaching skills", Indian journal of Teacher Education ANWESHIKA, NCTE, New Delhi, vol. 6 No.2 p.57-74. | Chambers, J.A.and Sprecker, J.W.(1993), Computer-Assisted Instruction: Its Use in the classroom, Prentice-Hall, New Jersey. | Criswell,E.L (1989). The design of computer- based Instruction. New York: Basic Books. | Curriculum Development Center (2003a) .Teaching Courseware: English Language -Form one. Ministry of Education. Malaysia.